This article has been accepted for publication in a future issue of this journal, but has not been fully edited. Content may change prior to final publication. Citation information: DOI 10.1109/TNB.2016.2560764, IEEE Transactions on NanoBioscience

Implementing Nonlinear Feedback Controllers using DNA Strand Displacement Reactions

Rucha Sawlekar[1], Francesco Montefusco[2], Vishwesh V. Kulkarni[1] and Declan G. Bates[1]

***Abstract*—We show how an important class of nonlinear feedback controllers can be designed using idealized abstract chemical reactions and implemented via DNA strand displacement (DSD) reactions. Exploiting *chemical reaction networks* (CRNs) as a programming language for the design of complex circuits and networks, we show how a set of unimolecular and bimolecular reactions can be used to realize input-output dynamics that produce a nonlinear *quasi sliding mode* (QSM) feedback controller. The kinetics of the required chemical reactions can then be implemented as enzyme-free, enthalpy/entropy driven DNA reactions using a toehold mediated strand displacement mechanism via Watson-Crick base pairing and branch migration. We demonstrate that the closed loop response of the nonlinear QSM controller outperforms a traditional linear controller by facilitating much faster tracking response dynamics without introducing overshoots in the transient response. The resulting controller is highly modular and is less affected by retroactivity effects than standard linear designs.**

***Index Terms*—Sliding mode control, DNA strand displacement, chemical reaction networks, saturation nonlinearity, retroactivity.**

I. INTRODUCTION

SEVERAL of the proposed industrial and biomedical applications of synthetic biology require the ability to precisely and robustly control the behaviour of synthetic circuits or devices at a biomolecular level [1], [2]. A fundamental aim of synthetic biology is thus to achieve the capability to design and implement robust embedded biomolecular feedback control circuits [3]. One appropriate modelling and design framework for tackling this problem is provided by *chemical reaction networks* (CRNs), which represent a convenient and concise approach to modelling chemical and biological processes, as well as an effective tool for the analysis of their behaviour from both deterministic [4], [5] and stochastic [6], [7] viewpoints. Previous work on the implementation of feedback controllers using DNA within this framework has focussed on the design of linear time-invariant systems only, e.g. the *proportional+integrator* (PI) controllers described in [8], [9], [10]. This approach fails to exploit the inherent potential of biomolecular circuits to implement nonlinear dynamical systems [11], [12], [13], and also requires the use of additional circuitry to overcome the wind-up effects associated with the integrator action.

[1]Rucha Sawlekar, Vishwesh Kulkarni and Declan Bates are with the Warwick Centre for Integrative Synthetic Biology (WISB), School of Engineering, University of Warwick, Coventry, CV4 7AL, United Kingdom e-mail: R.Sawlekar@warwick.ac.uk, V.Kulkarni@warwick.ac.uk, D.Bates@warwick.ac.uk.

[2]Francesco Montefusco is with the Department of Information Engineering, University of Padova, Padova 35131 e-mail: montefusco@dei.unipd.it.

In this paper, we extend the approach of [8], [9], [10] to allow the implementation of nonlinear feedback controllers. We focus on a well-known type of nonlinear controller called a *sliding mode controller* (SMC), whose strong performance and robustness characteristics have been widely recognised in more traditional control engineering applications [14], [15]. From sliding mode control theory, a perfect SMC can be represented by a relay nonlinearity (see [14], [16], [17]). To avoid a number of theoretical and practical issues with the implementation of such discontinuous switches, in engineering practice SMC's are usually implemented as *quasi sliding mode* (QSM) controllers, i.e. continuous/smooth approximations of the discontinuous SMC. Here, we show how a set of irreversible chemical reactions can provide a biomolecular implementation of a nonlinear QSM controller. We show how the kinetics of the required chemical reactions can then be implemented as enzyme-free, entropy/enthalpy driven DNA reactions [18], using strand displacement as an elementary computational mechanism.

We implement this controller on a prototype embedded closed loop feedback system that consists of three individual modules, a subtractor, a controller and a biomolecular process to be controlled, each realized by mass action kinetics at a molecular level and interconnected using a modular approach as shown in Fig. 1. In contrast to previous implementations of DNA-based feedback controllers, the biomolecular process to be controlled here is both dynamic and nonlinear. Note also that the subtractor module must be represented as a dynamical system, unlike in standard feedback control systems which assume the availability of an ideal subtractor. Analysis of the closed loop performance of the QSM controller reveals significant performance advantages compared to a linear PI controller, particularly when retroactivity effects (see [19], [20], and [21]) are taken into account.

The manuscript is organised as follows. In section II we present background results on how to implement linear systems in the proposed framework. In section III, we present our main results on how to realize a nonlinear quasi sliding mode controller using chemical reaction networks and DNA strand displacement reactions. In section IV, we present simulation results for our prototype closed loop system that demonstrate the superior performance obtained with the quasi sliding mode controller, compared to a traditional PI controller. We offer some conclusions and discuss directions for future research in Section V and tabulate all necessary chemical reactions and DNA computations in the Appendix. An early version of this paper appeared in [22].

This article has been accepted for publication in a future issue of this journal, but has not been fully edited. Content may change prior to final publication. Citation information: DOI 10.1109/TNB.2016.2560764, IEEE Transactions on NanoBioscience

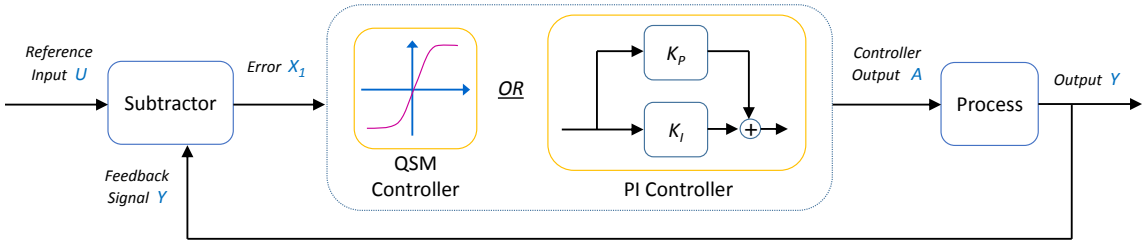

Fig. 1: A prototype embedded biomolecular closed loop feedback control system

II. Recent Work

Our notation follows that used in [8] and [9]: for example, we represent a bidirectional, i.e. reversible, bimolecular chemical reaction as:

$$X_1 + X_2 \underset{k_2}{\overset{k_1}{\rightleftharpoons}} X_3 + X_4,$$

where, X_i are chemical species with X_1 and X_2 being the reactants and X_3 and X_4 being the products. Here, k_1 denotes the forward reaction rate and k_2 denotes the backward reaction rate. A unimolecular reaction features only one reactant whereas a multimolecular reaction features two or more reactants. Degradation of a chemical species X at rate k into a waste product or an inert form is denoted as $X \xrightarrow{k} \emptyset$.

A. DNA strand displacement mechanism

We now present a brief overview of the DNA Strand Displacement (DSD) mechanism (see [23] and [24]) through which the types of idealized chemical reactions used in this paper may be implemented. Consider the reversible bimolecular reaction:

$$X + P \underset{k_{ub}}{\overset{k_b}{\rightleftharpoons}} Y + Q, \tag{1}$$

where, X, P, Y and Q are DNA strands while k_b and k_{ub} are the binding and unbinding rates, respectively. A DSD implementation of this reaction is shown in Fig. 2. It begins with an invader strand P binding to the complementary target strand X at the toehold **1*** through Watson-Crick base pairing [27]. Through an intermediate process of *branch migration*, P displaces the evader strand **2-3** from X, thereby producing the partially double stranded product Y that can further react with other DNA complexes using the toehold **3***.

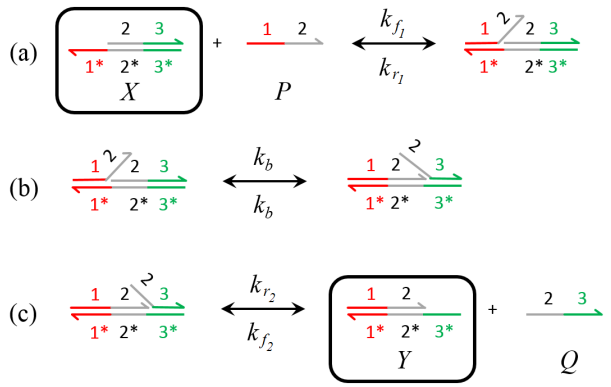

Fig. 2: Examples of DNA strand displacement reactions illustrated using the software package Visual DSD [25] : the DNA strands are bonded by Watson-Crick base pairing, denoted by * and the basic steps involved are (a) binding of toehold **1** to **1***, (b) branch migration wherein the strand **1-2** partially displaces strand **2-3**, and (c) complete separation of strand **2-3** [26].

If DNA strands belong to entirely different domains, as is often the case, they do not interact with each other directly and therefore DSD reactions must be mediated by so-called auxiliary DNA species, which must be present in sufficiently large amounts [26]. We assume that complementary strands react only with each other, although this constraint can be relaxed, as demonstrated in [10]. For the DSD reactions to be fast and thereby reduce mismatches during branch migrations, the toehold domains should be short: for example, of the order of 6–10 nt, where *nt* denotes nucleotides, and the displacement domains should preferably be 20 nt [28]. The reaction rate constants, and consequently the kinetics of the system, are a function of the toehold binding strength and can thus be altered by varying the binding strength and the strand composition [26]. Elementary DNA reactions are approximated into CRNs by excluding auxiliary species as described in [11] (see Appendix). Corresponding reaction rates are also approximated in terms of initial concentration of auxiliary DNA species (C_{max}), and forward binding reaction rates (q_i and q_{max}).

B. Representing linear systems using idealized chemical reactions

Linear time-invariant (LTI) systems can be realized using three types of operations: integration, summation, and multiplication by a constant. Here we summarise previous results on how such systems can be realized using idealized chemical reactions.

Whereas signals in systems theory can take both positive and negative values, biomolecular concentrations can only take non-negative values. To resolve this difficulty, we follow the approach in [8] and [9], and represent a signal x as the difference in concentrations of two DNA strands. Here, x^+ and x^- are respectively the positive and negative components of x such that $x = x^+ - x^-$. As an example, consider Fig. 3, where a DNA strand x^+ with a concentration of 10 nM is added at time $t = 0$s. When DNA strand x^- is added with a concentration of 20 nM at time $t = 20,000$s, the value of the signal x changes from positive to negative.

This article has been accepted for publication in a future issue of this journal, but has not been fully edited. Content may change prior to final publication. Citation information: DOI 10.1109/TNB.2016.2560764, IEEE Transactions on NanoBioscience

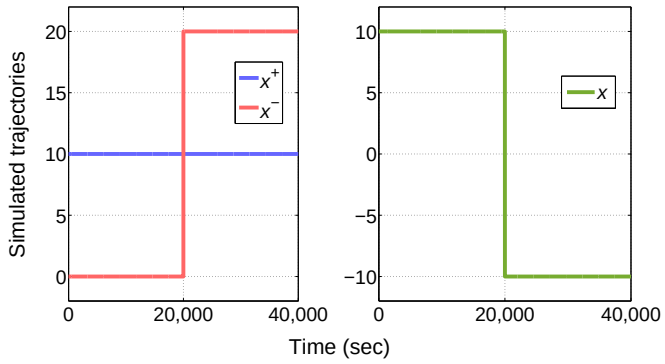

Fig. 3: The square wave signal (right) is generated by two instantaneous additions of chemical species at $t = 0,\ 20,000$s using the relation $x(t) = x^+(t) - x^-(t)$. DNA strand x^+ is added at time $t = 0$ with x^- being absent (left) resulting in a positive value of the signal x for $t \in [0, 20,000)$s. Later, DNA strand x^- is added at time $t = 20,000$s resulting in the signal x becoming negative for $t \in [20,000, 40,000)$s.

In [8], results on how to represent elementary system theoretic operations such as gain, summation and integration using idealized abstract chemical reactions were obtained and it is shown that only three types of elementary chemical reactions, namely, catalysis, annihilation and degradation are needed for such representations. In [9], this set of elementary chemical reactions was further reduced to only two. We now summarise the main results and refer the interested reader to [8] and [9] for the complete background theory.

Strictly speaking, each of the below equations with superscript $\pm$ and $\mp$ should be written down after decomposing them into their '+' and '−' individual components - for example, $x_i^{\pm} \xrightarrow{k} x_o^{\pm}$ should be written as the set of the following two reactions: $x_i^{+} \xrightarrow{k} x_o^{+}$ and $x_i^{-} \xrightarrow{k} x_o^{-}$. However, for brevity, following [8], we will represent such a set of reactions compactly as $x_i^{\pm} \xrightarrow{k} x_o^{\pm}$.

Lemma 1: [Scalar gain K]
Let $x_o = Kx_i$ where x_i is the input, x_o is the output and K is the gain. This operation is implemented using the following set of abstract chemical reactions: $x_i^{\pm} \xrightarrow{\gamma K} x_i^{\pm} + x_o^{\pm}$, $x_o^{\pm} \xrightarrow{\gamma} \emptyset$ and $x_o^{+} + x_o^{-} \xrightarrow{\eta} \emptyset$, where γ and η are the kinetic rates associated with degradation and annihilation respectively.

Lemma 2: [Summation]
Consider the summation operation $x_o = x_i + x_d$, where x_i and x_d are the inputs and x_o is the output. This operation is implemented using the following set of abstract chemical reactions: $x_i^{\pm} \xrightarrow{\gamma} x_i^{\pm} + x_o^{\pm}$, $x_d^{\pm} \xrightarrow{\gamma} x_d^{\pm} + x_o^{\pm}$, $x_o^{\pm} \xrightarrow{\gamma} \emptyset$ and $x_o^{+} + x_o^{-} \xrightarrow{\eta} \emptyset$. The subtraction operation $x_o = x_i - x_d$ is implemented using the following set of abstract chemical reactions: $x_i^{\pm} \xrightarrow{\gamma} x_i^{\pm} + x_o^{\pm}$, $x_d^{\pm} \xrightarrow{\gamma} x_d^{\pm} + x_o^{\mp}$, $x_o^{\pm} \xrightarrow{\gamma} \emptyset$ and $x_o^{+} + x_o^{-} \xrightarrow{\eta} \emptyset$.

Lemma 3: [Integration]
Consider the integrator $x_o = K \int x_i dt$ where, x_i is the input, x_o is the output, and K is the DC gain. This operation is implemented using the following set of abstract chemical reactions: $x_i^{\pm} \xrightarrow{K} x_i^{\pm} + x_o^{\pm}$ and $x_o^{+} + x_o^{-} \xrightarrow{\eta} \emptyset$.

Using generalised mass-action kinetics, it follows that the gain operator realized in this manner is described using the ODE, $\frac{dx_o}{dt} = \gamma(Kx_i - x_o)$. Likewise, the ODEs for the summation and integrator operations are given by $\frac{dx_o}{dt} = \gamma(x_i + x_d - x_o)$ and $\frac{dx_o}{dt} = Kx_i$, respectively.

III. Main Results

We now present our main results on how the closed loop system modules shown in Fig. 1 can be synthesized individually using DNA strand displacement reactions.

A. Quasi sliding mode controller

Taking inspiration from the ultrasensitive input-output behaviour exhibited by *mitogen-activated protein kinases* (MAPK) signaling cascades, [29], [30], [31], we now present a set of idealized chemical reactions that can be used to generate switch-like input-output responses. When implemented as elementary DNA reactions, for example by using the software package Visual DSD [25], these reactions can be used to construct a nonlinear QSM feedback controller. Consider the following set of idealized CRNs, where the signal X_1 is the input of the system and the signal A is the output, $X_1 = X_1^+ - X_1^-$ and $A = A^+ - A^-$, respectively, and the strands X_1^+, X_1^- and A^+, A^- have a free toehold each:

$$X_1^{\pm} + B^{\pm} \xrightarrow{k_{b_1}} X_2^{\pm}, \tag{2a}$$
$$X_2^{\pm} \xrightarrow{k_{c_1}} A^{\pm} + X_1^{\pm}, \tag{2b}$$
$$X_2^{+} + X_2^{-} \xrightarrow{\eta} \phi, \tag{2c}$$
$$A^{+} + A^{-} \xrightarrow{\eta} \phi, \tag{2d}$$
$$A^{\pm} + X_3^{\pm} \xrightarrow{k_{b_2}} X_4^{\pm}, \tag{2e}$$
$$X_4^{\pm} \xrightarrow{k_{c_2}} B^{\pm} + X_3^{\pm}, \tag{2f}$$
$$X_4^{+} + X_4^{-} \xrightarrow{\eta} \phi, \tag{2g}$$
$$B^{+} + B^{-} \xrightarrow{\eta} \phi. \tag{2h}$$

The above CRNs realize an ultrasensitive switch-like input-output response, as illustrated in Fig. 4. By tuning the concentration of the DNA strands $X_3^{\pm}$, the input-output response of the set of CRNs can be made to closely approximate the ideal switch implemented by a SMC, i.e. the set of CRNs (2) implements a QSM controller. Here, k_{b_1} and k_{b_2} denote the binding reaction rates whereas k_{c_1} and k_{c_2} denote the catalytic reaction rates.

The CRNs (2) are approximations of elementary DNA reactions which can be realized using Visual DSD software, [25], as illustrated in Figs. 5, 6 and 9. The DSD implementation of the catalysis reactions given by (2b) and (2f) is shown in Fig. 5. Accordingly, the reactions (2b), (2f) initiate with the *single strand DNA* (ssDNA) $X_2^{\pm}$ (or $X_4^{\pm}$) displacing auxiliary species $G_i^{\pm}$ irreversibly at the rate q_i, producing the intermediate complex $O_i^{\pm}$ and waste. Complex $O_i^{\pm}$ on reacting with auxiliary species $T_i^{\pm}$, releases two single stranded products, $A^{\pm}$ (or $B^{\pm}$) and $X_1^{\pm}$ (or $X_3^{\pm}$). The DSD implementation of the bimolecular reactions (2a) and (2e) is shown in Fig 6. Here,

This article has been accepted for publication in a future issue of this journal, but has not been fully edited. Content may change prior to final publication. Citation information: DOI 10.1109/TNB.2016.2560764, IEEE Transactions on NanoBioscience

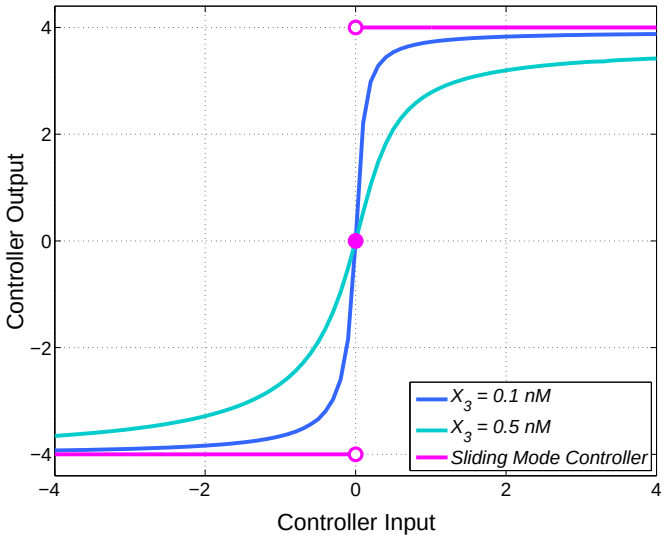

Fig. 4: Input-output characteristics of an ideal sliding mode controller and quasi sliding mode controller for different values of the tuning parameter X_3.

the reaction begins with single strand $X_1^{\pm}$ (or $A^{\pm}$) reacting reversibly with the auxiliary species $L_i^{\pm}$ to produce activated intermediate complexes $H_i^{\pm}$ and $B_i^{\pm}$. Due to the presence of $X_1^{\pm}$ (or $X_3^{\pm}$) in the solution with an active toehold, it reacts with complex $H_i^{\pm}$ to release intermediate complex $O_i^{\pm}$. If $X_1^{\pm}$ is absent then $B_i^{\pm}$ can reversibly displace $H_i^{\pm}$, releasing $X_1^{\pm}$ back into the solution. Complex $O_i^{\pm}$ displaces $T_i^{\pm}$. Hence, the bimolecular reactions given by (2a) and (2e) are irreversible and produce ssDNA products $X_2^{\pm}$ and $X_4^{\pm}$, respectively. The full set of elementary DNA reactions required to realize the QSM controller are given in the appendix.

Now, using mass action kinetics, the set of reactions given by (2) may be represented by the following set of ODEs:

$$\frac{dA}{dt} = k_{c_1}X_2 - k_{b_2}AX_3, \tag{3a}$$
$$\frac{dX_2}{dt} = k_{b_1}X_1B - k_{c_1}X_2, \tag{3b}$$
$$\frac{dB}{dt} = -k_{b_1}X_1B + k_{c_2}X_4, \tag{3c}$$
$$\frac{dX_4}{dt} = k_{b_2}AX_3 - k_{c_2}X_4. \tag{3d}$$

where, X_1 is the input and A is the output of the QSM controller. From equations (3a) to (3d) we can see that $A + B + X_2 + X_4 = \text{constant} \doteq S_{qsm}$. Thus the signal B is variable and depends on the dynamic signals A, X_2, X_4. Since, X_1 also varies over time this means that the term $k_{b_1}X_1B$ in (3b) is nonlinear. It can be checked that:

$$\frac{dX_2^+}{dt} = k_{b_1}X_1^+B^+ - k_{c_1}X_2^+ - \eta X_2^+X_2^-, \tag{4}$$
$$\frac{dX_2^-}{dt} = k_{b_1}X_1^-B^- - k_{c_1}X_2^- - \eta X_2^+X_2^-. \tag{5}$$

Hence,

$$\begin{aligned}\frac{dX_2}{dt} &= \frac{dX_2^+}{dt} - \frac{dX_2^-}{dt}\\ &= (k_{b_1}X_1^+B^+ - k_{c_1}X_2^+ - \eta X_2^+X_2^-)\\ &\quad -(k_{b_1}X_1^-B^- - k_{c_1}X_2^- - \eta X_2^+X_2^-)\\ &= k_{b_1}\{(X_1^+B^+) - (X_1^-B^-)\} - k_{c_1}(X_2^+ - X_2^-)\\ &= k_{b_1}\{(X_1B)^+ - (X_1B)^-)\} - k_{c_1}X_2,\end{aligned}$$

where, $X_1^+B^+ = (X_1B)^+$ and $X_1^-B^- = (X_1B)^-$. Hence,

$$\frac{dX_2}{dt} = k_{b_1}X_1B - k_{c_1}X_2.$$

Now, from sliding mode control theory, a perfect SMC can be represented by a relay nonlinearity (see [14], [16], [17]). As shown in Fig. 4, this can be obtained as the limiting case of a controller implemented using the equations (3a) - (3d). For example, as $X_3 \to 0$, the output A of the controller can be described by the following relay-type saturation nonlinearity (see Fig. 4):

$$A(t) = k_{SMC} \cdot \text{sgn}(X_1(t)), \tag{6}$$

where $\text{sgn}(\cdot)$ denotes the signum function and $X_1(t)$ is the input to the controller (the error signal generated by the subtractor). Such a controller has a discontinuity on the straight line $X_1 = 0$ which is traditionally referred to as the *sliding manifold* $\sigma \stackrel{def}{=} X_1 = 0$, where σ is the sliding variable. The control signal A, defined by (6), is therefore designed to force the system to move toward the sliding manifold $\sigma = 0$ (the *reaching phase* of SMC) and then maintain this condition (i.e. $\sigma = 0$) for all future time (the *sliding phase* of SMC).

In practice, however, implementations of perfect sliding mode controllers cause the system's closed loop response to exhibit a zigzag motion of small amplitude and high frequency, due to imperfections in switching devices and delays [14], [16], [17]. This effect, known as *chattering*, is typically avoided by using continuous/smooth approximations of the discontinuous SMC, resulting in a so-called *quasi sliding mode* (QSM) controller.

The controller implemented using equations (3a) - (3d) is an example of such a function, since it approximates the nonlinearity $\text{sgn}(X_1)$. Since with a QSM controller there is no ideal sliding mode in the closed loop system, the sliding variable (error) cannot be driven exactly to zero in a finite time, [14]. However, if our QSM controller is made more ultrasensitive (for example, by decreasing X_3), the input-output behaviour of our QSM controller approaches the limiting case of an ideal SMC, as illustrated in Fig. 4, and the error signal can be made as small as desired.

B. Nonlinear process to be controlled

To act as a challenging benchmark control problem, we select a process composed of both unimolecular and bimolec-

This article has been accepted for publication in a future issue of this journal, but has not been fully edited. Content may change prior to final publication. Citation information: DOI 10.1109/TNB.2016.2560764, IEEE Transactions on NanoBioscience

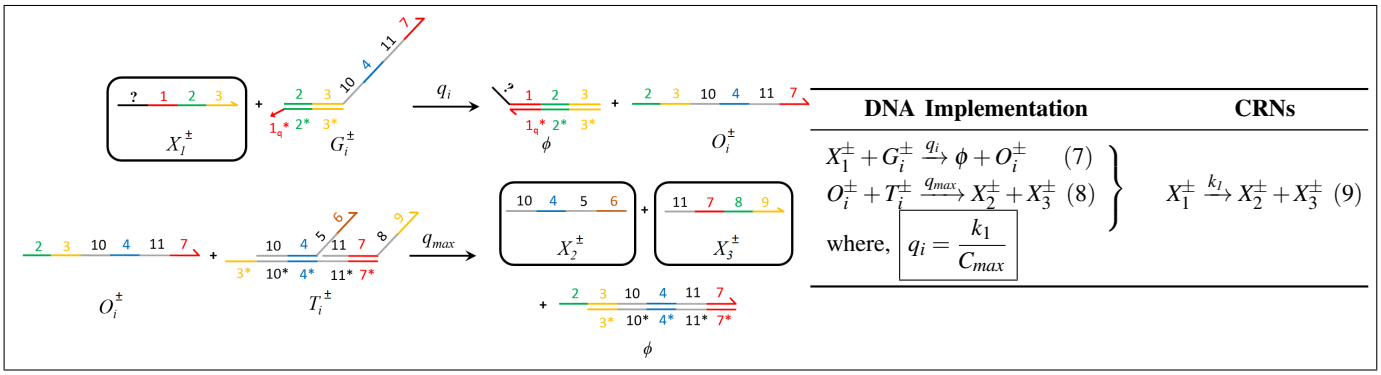

Fig. 5: Catalysis reaction $X_1^{\pm} \rightarrow X_2^{\pm} + X_3^{\pm}$. The DNA implementation with reaction index i corresponding to the unimolecular CRN using signal species $X_1^{\pm}$, $X_2^{\pm}$ and $X_3^{\pm}$ highlighted in black boxes. Domain 1_q^* may not be entirely complement of domain **1** but its toehold domain reaction rate is tuned to q_i. In (16), species G_i reacts with X to displace O_i and in (17), O_i releases X and Y, on reacting with species T_i [11]. The question mark appearing on the DNA strands such as X_1 and ϕ, indicates species identifier; as adapted from [8].

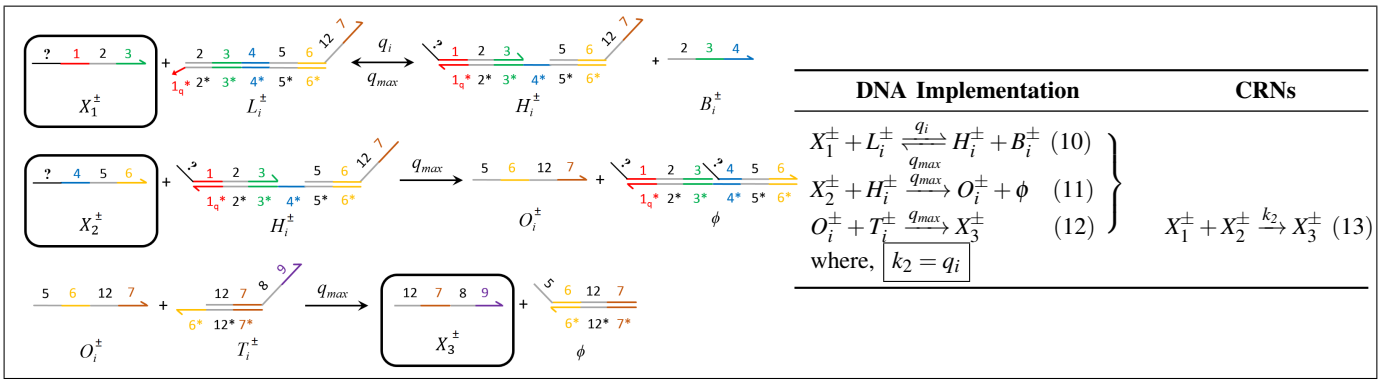

Fig. 6: Bimolecular CRN $X_1^{\pm} + X_2^{\pm} \xrightarrow{k_2} X_3^{\pm}$: DNA implementation of bimolecular CRN (13) with reaction index i and black boxes highlighting the formal species, $X_1^{\pm}$, $X_2^{\pm}$, $X_3^{\pm}$ that appear in the approximated CRN. In (10) $X_1^{\pm}$ displaces auxiliary species $L_i^{\pm}$ reversibly producing intermediate complex $H_i^{\pm}$ which reacts with $X_2^{\pm}$ as given in (11) producing $O_i^{\pm}$. In (12), $X_3^{\pm}$ is produced when $O_i^{\pm}$ irreversibly displaces $T_i^{\pm}$; as adapted from [11].

ular reactions, given as follows, whose dynamics are to be controlled:

$$A^{\pm} + X_5^{\pm} \xrightarrow{k_{r_1}} X_6^{\pm}, \tag{14a}$$
$$X_6^{\pm} \xrightarrow{k_{r_2}} Y^{\pm} + X_5^{\pm}, \tag{14b}$$
$$Y^{\pm} \xrightarrow{k_{r_3}} \phi, \tag{14c}$$
$$Y^{+} + Y^{-} \xrightarrow{\eta} \phi. \tag{14d}$$

Here, the process input is the ssDNA $A^{\pm}$ and the process output is the ssDNA $Y^{\pm}$. k_{r_1} is a binding reaction rate, k_{r_2} is the catalytic reaction rate, and k_{r_3} is the degradation rate. These reaction rates and their values are as listed in Table II.

This process was chosen because application of standard Michaelis-Mentens kinetics to these reactions results in a set of ODEs with nonlinear response dynamics, given by:

$$\frac{dX_5}{dt} = -k_{r_1} A X_5 + k_{r_2} X_6, \tag{15a}$$
$$\frac{dX_6}{dt} = k_{r_1} A X_5 - k_{r_2} X_6, \tag{15b}$$
$$\frac{dY}{dt} = k_{r_2} X_6 - k_{r_3} Y. \tag{15c}$$

From (15), we can conclude that $X_{Total} \doteq X_5 + X_6$ is conserved through the lifetime of the process and have therefore set it to a constant value, as noted in Table II. In the context of our feedback system shown in Fig. 1, the process input signal is the controller output A and the process output signal Y is fed back as an input signal to the subtractor. In the control literature it is well known that nonlinear systems are in general more difficult to control than linear systems. Also, previous work on the implementation of linear feedback controllers using nucleic acids considered only a static process to be controlled [8], [9], [10]. The system described here

This article has been accepted for publication in a future issue of this journal, but has not been fully edited. Content may change prior to final publication. Citation information: DOI 10.1109/TNB.2016.2560764, IEEE Transactions on NanoBioscience

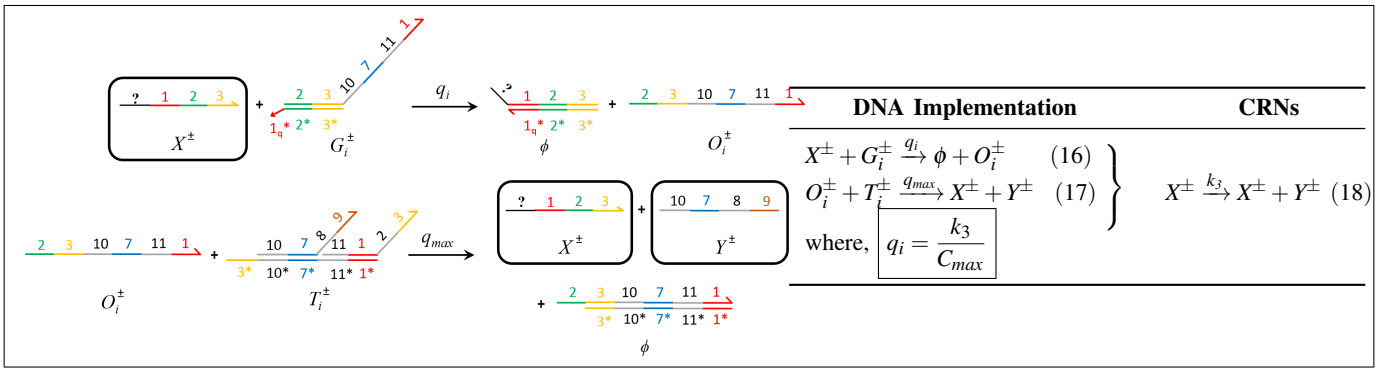

Fig. 7: Catalysis reaction $X^{\pm} \rightarrow X^{\pm} + Y^{\pm}$. The unimolecular catalysis CRN (18) is approximated from the DNA implementation with reaction index i. The signal species are $X^{\pm}$ and $Y^{\pm}$. In (16), species $G_i^{\pm}$ reacts with $X^{\pm}$ to produce $O_i^{\pm}$ and in (17), $O_i^{\pm}$ releases $X^{\pm}$ and $Y^{\pm}$, on reacting with species $T_i^{\pm}$; as adapted from [8]. The strand displacement mechanism resembles that in Fig. 5 but, the nucleotide composition of product species vary depending on the composition of auxiliary species involved [11].

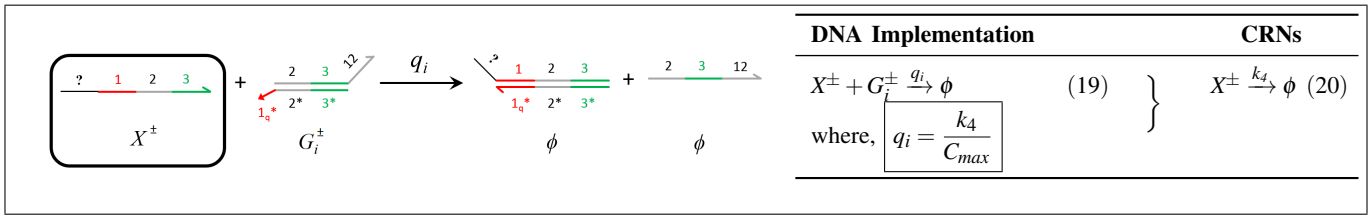

Fig. 8: Degradation reaction $X^{\pm} \xrightarrow{k_4} \phi$: DNA implementation of formal species $X^{\pm}$ degradation on reacting with auxiliary species G_i. In (19), $X^{\pm}$ performs strand displacement on G_i producing inert waste. (20) represents the CRN derived from the formal DNA strand displacement reaction (19); as adapted from [8].

represents the first attempt to design a feedback controller for a biomolecular process which is both dynamic and nonlinear.

C. Subtractor

Following [8] and [10], we implement the subtraction $U - Y$ of two signals U and Y. The subtraction operation can be achieved using the following set of reactions:

$$U^{\pm} \xrightarrow{k_s} U^{\pm} + X_1^{\pm}, \tag{21a}$$
$$Y^{\pm} \xrightarrow{k_s} Y^{\pm} + X_1^{\mp}, \tag{21b}$$
$$X_1^{\pm} \xrightarrow{k_s} \phi, \tag{21c}$$
$$X_1^{+} + X_1^{-} \xrightarrow{\eta} \phi. \tag{21d}$$

Here, signals U and Y are the inputs and X_1 is the output of the subtractor. In other words, the value of signal X_1 being produced is equivalent to that of the difference between the two input signals, U and Y. In addition, both the catalysis reaction rates in (21a)-(21b) are set to be equal to the degradation rate. Note that this subtractor module is itself a dynamical system and produces the desired result, i.e., subtraction of the two input signals, as its steady-steady output. Applying mass action kinetics to (21) gives:

$$\frac{dX_1}{dt} = k_s(U - Y - X_1). \tag{22}$$

By choosing a higher value of k_s, the response of the subtractor can be speeded up so that the required steady-state value $U - Y$ is computed more rapidly. More details of the subtraction operator can be found in [8] and [10]. In the context of our feedback system shown in Fig. 1, the inputs to the subtractor comprise the reference input signal U and the plant output Y while its output X_1 is fed as the input to the controller.

D. PI controller

For the purposes of evaluating the performance of our nonlinear QSM controller, we also implement a linear PI controller [33], [34]. Following the approach of [8] and [10], we obtain the following representation for the PI controller — our CRNs are slightly different from the ones given in [8] and [10] because they have been optimized for the feedback system illustrated in Fig. 1. The PI controller is made up of an integrator implemented via the reactions:

$$X_1^{\pm} \xrightarrow{k_I} X_1^{\pm} + X_2^{\pm}, \tag{23a}$$
$$X_2^{+} + X_2^{-} \xrightarrow{\eta} \phi. \tag{23b}$$

This article has been accepted for publication in a future issue of this journal, but has not been fully edited. Content may change prior to final publication. Citation information: DOI 10.1109/TNB.2016.2560764, IEEE Transactions on NanoBioscience

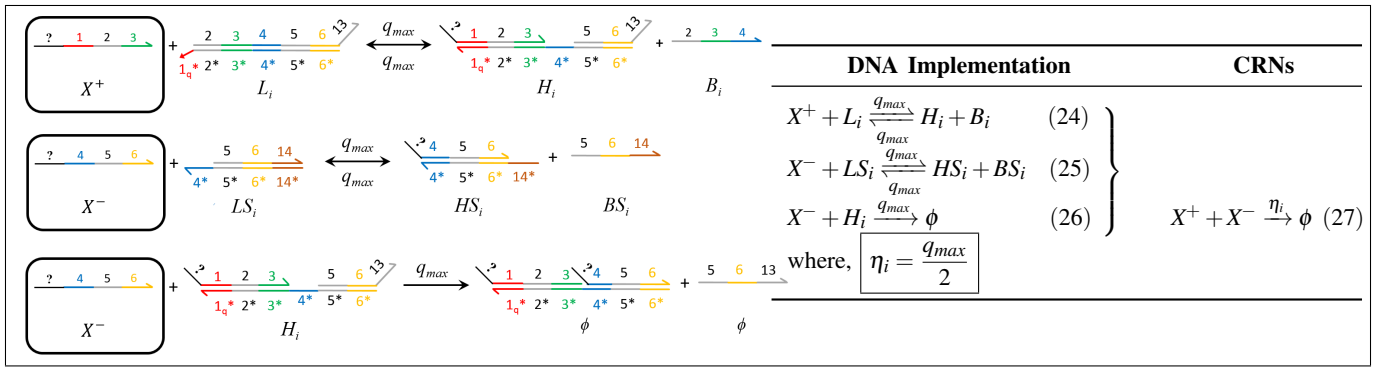

Fig. 9: Annihilation reaction $X^+ + X^- \xrightarrow{\eta_i} \phi$: The DSD diagram shows degradation of auxiliary species X^+ and X^- by means of molecules L_i and LS_i. The reaction dynamics are separated into fast and slow time scales such that, X^+ and X^- are sequestered into intermediate species through reaction with L_i and LS_i at a fast reaction rate, while X^- degrades into waste by reacting with H_i at a slower rate. The initial concentrations of X^+ and X^- must be scaled by a factor of 2 (let, $\xi = 2$, hence, $X_0^+ = 1\xi$ nM and $X_0^- = 0.5\xi$ nM) to attenuate for the sequestering effect of the fast dynamics; as adapted from [8].

and a proportional gain, implemented as:

$$X_1^{\pm} \xrightarrow{k_p} X_1^{\pm} + A^{\pm}, \tag{28a}$$
$$X_2^{\pm} \xrightarrow{k_c} X_2^{\pm} + A^{\pm}, \tag{28b}$$
$$A^{\pm} \xrightarrow{k_d} \phi, \tag{28c}$$
$$A^{+} + A^{-} \xrightarrow{\eta} \phi. \tag{28d}$$

Here, the signal X_1 is the input and A is the output. Furthermore, k_p and k_c denote the catalytic reaction rates while k_d denotes the degradation rate. The values of these rates are given in Table III. Using mass action kinetics, the following ODE representation is obtained for the PI controller:

$$\frac{dX_2}{dt} = k_I X_1, \tag{29}$$
$$\frac{dA}{dt} = k_p X_1 + k_c X_2 - k_d A. \tag{30}$$

E. DNA implementations

The linear components of the feedback control system, i.e. the subtractor and PI controller [8], are built using a combination of catalysis–Fig. 7, degradation–Fig. 8 and annihilation–Fig. 9 reactions. The nonlinear components, i.e. the QSM controller and the process to be controlled are constructed based on catalysis–Fig. 5 and bimolecular–Fig. 6 reactions.

Note that the catalysis reactions (9) and (18) in Figs. 5 and 7, respectively, produce different output species depending on the domain composition of the reactant auxiliary species. Species $G_i^{\pm}$ and $T_i^{\pm}$, which are partially double stranded DNAs, and single strands of $O_i^{\pm}$, can be observed to have different domain compositions in Fig. 5 and Fig. 7. As a result, in (9) two different products, $X_2^{\pm}$ and $X_3^{\pm}$, are obtained whereas, in (18) the single species $X^{\pm}$ is reproduced.

The domain 1_q^* in Figs. 5–9 denotes the subsequence of domain 1 that may be the same length as 1 but contains some mismatched bases over the displacement domain. The reaction rate of 1_q^* is however tuned to rate q_i [11] and other corresponding reaction rates are set by following the notation from [8] and [11]. Initial concentrations of the auxiliary species $G_{i_0}^{\pm}$, $T_{i_0}^{\pm}$, $L_{i_0}^{\pm}$, $B_{i_0}^{\pm}$, $LS_{i_0}^{\pm}$, $BS_{i_0}^{\pm}$ are set to $C_{max} = 1000$ nM. In Fig. 6, which gives the DNA implementation of the bimolecular CRN, the concentrations of $T_i^{\pm}$, $L_i^{\pm}$, $B_i^{\pm}$ remain constant throughout the process [11]. All the other initial concentrations for the remaining species are set to zero.

The rest of this manuscript investigates the closed loop performance properties of the QSM controller, when compared with a linear time-invariant controller synthesized according to the methodologies proposed in [8] and [10]. We re-emphasize that the distinguishing feature of our nonlinear controller (and process to be controlled) is the use of bimolecular reactions; the linear time-invariant systems synthesized in [8] and [10] use unimolecular reactions only.

IV. SIMULATION RESULTS

In the following simulations, all reaction rates and total substrate values have been set to the nominal values given in Table I to III. The second order reaction rates are tuned within the practical experimental limits (a maximum value of 10^7 /M/s) and catalysis, degradation, annihilation rates have been chosen in terms of DNA implementation reaction rates, q_i and initial concentration of auxiliary species, C_{max}.

	Parameters	Nominal Values
S_{qsm}	total substrate	4 nM
X_3	tuning parameter	0.1 nM
k_{b_1}	forward binding rate	10^7 /M/s
k_{b_2}	forward binding rate	10^7 /M/s
k_{c_1}	catalytic reaction rate	100 q_i C_{max} /s
k_{c_2}	catalytic reaction rate	50 q_i C_{max} /s

TABLE I: QSM controller — parameter values

This article has been accepted for publication in a future issue of this journal, but has not been fully edited. Content may change prior to final publication. Citation information: DOI 10.1109/TNB.2016.2560764, IEEE Transactions on NanoBioscience

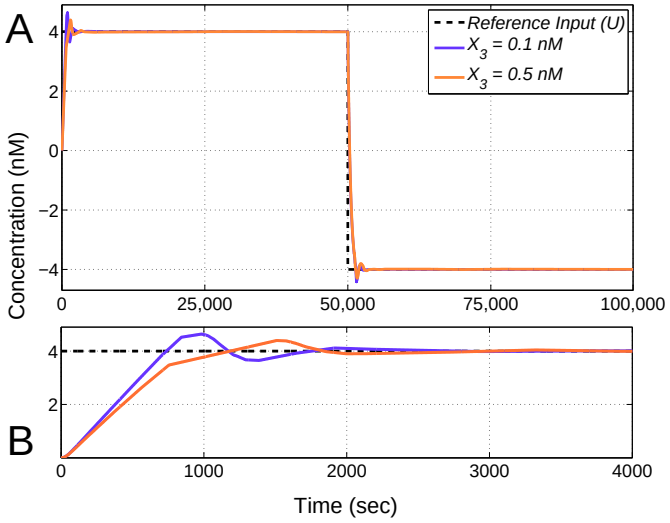

Fig. 10: Closed loop tracking response obtained using the QSM controller. Here, the reference input U is a square wave of magnitude 4 nM. The transient response can be made faster by reducing the controller tuning parameter X_3. The subfigure "B" is a zoomed-in version of the subfigure "A" to better illustrate the transient response in the region of interest.

Initial values of the signals A, B, X_2, X_4 are set to zero, i.e. $A_0 = B_0 = X_{2_0} = X_{4_0} = 0$ nM. For the PI controller, the nominal values of reaction rates and kinetic constants are shown in Table III and the initial concentrations of the non-auxiliary species in equations (23)-(28) are set to zero, i.e. $X_{2_0} = A_0 = 0$ nM. For the subtractor, k_s is set to its nominal value of $3000 \cdot q_i \cdot C_{max}$ /s where DNA implementation reaction rates $q_i = 800$ /M/s $(i = 1, 2, ..., 21)$, $q_{max} = 10^7$ /M/s and initial concentration of auxiliary species, $C_{max} = 1000$ nM. The reaction rate of annihilation, η, is set to $10 \cdot q_i C_{max}$ /s.

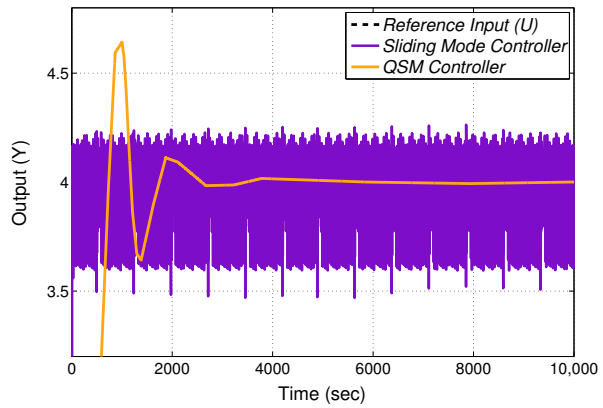

Fig. 11: Closed loop responses with quasi and ideal sliding mode controllers: the undesirable phenomenon of *chattering*, i.e., high frequency oscillations, is observed in the closed loop response if the ideal SMC controller is used, but is avoided by the QSM controller.

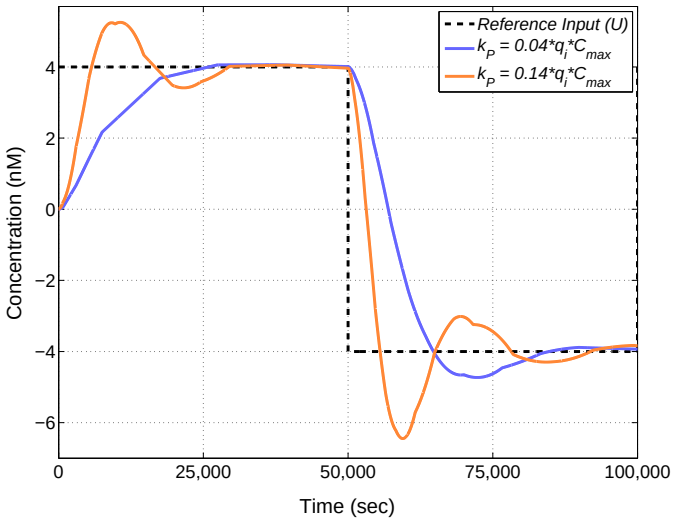

Fig. 12: Closed loop tracking response obtained using a PI controller. The transient response can be made faster by increasing the value of the controller tuning parameter k_P albeit at the cost of introducing progressively larger overshoots.

A square-wave input was chosen for the reference signal U to be tracked by the process output, in line with standard practice in control theory, since such signals generally result in the most challenging possible tracking problem for the control system (the output must track signals that are changing infinitely fast, in both directions). The magnitude of the square wave was chosen to be sufficiently large that it excites the nonlinear dynamics of the process to be controlled. Fig. 10 shows the closed loop tracking response for the system shown in Fig. 1 when the QSM controller is used. The output Y tracks the input U with a settling time of 2500s if X_3 is set to 0.1 nM . As shown in Fig. 11, the QSM controller also avoids the problem of chattering that is encountered when its limiting case, i.e., the ideal SMC, is used. Fig. 12 shows the closed loop tracking response for the system shown in Fig. 1 when

	Parameters	Nominal Values
k_{r_1}	forward binding rate	500×10^3 /M/s
k_{r_2}	catalytic reaction rate	2×10^3 q_i C_{max} /s
k_{r_3}	degradation rate	10×10^{-3} q_i C_{max} /s
X_{Total}	total amount of $X_5 + X_6$	3 nM

TABLE II: Process to be controlled — parameter values

	Parameters	Nominal Values
k_I	catalytic reaction rate	0.002 q_i C_{max} /s
k_P	catalytic reaction rate	0.04 q_i C_{max} /s
k_c	catalytic reaction rate	0.2 q_i C_{max} /s
k_d	degradation rate	0.4 q_i C_{max} /s

TABLE III: PI Controller — Parameter Values

This article has been accepted for publication in a future issue of this journal, but has not been fully edited. Content may change prior to final publication. Citation information: DOI 10.1109/TNB.2016.2560764, IEEE Transactions on NanoBioscience

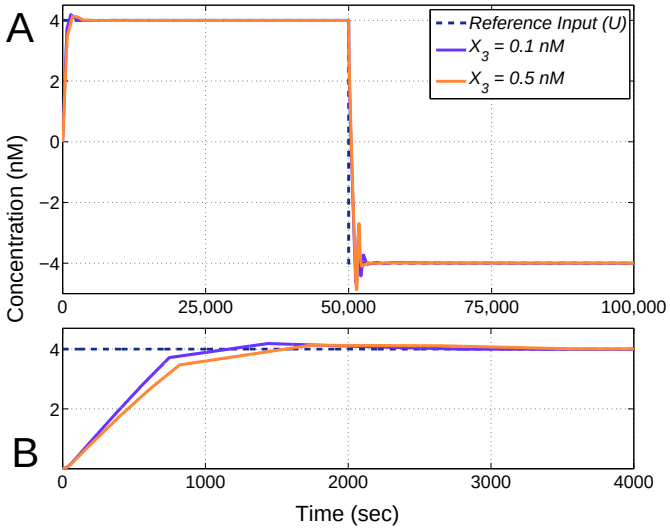

Fig. 13: Closed loop tracking response obtained by using the QSM controller after accounting for retroactivity effects.

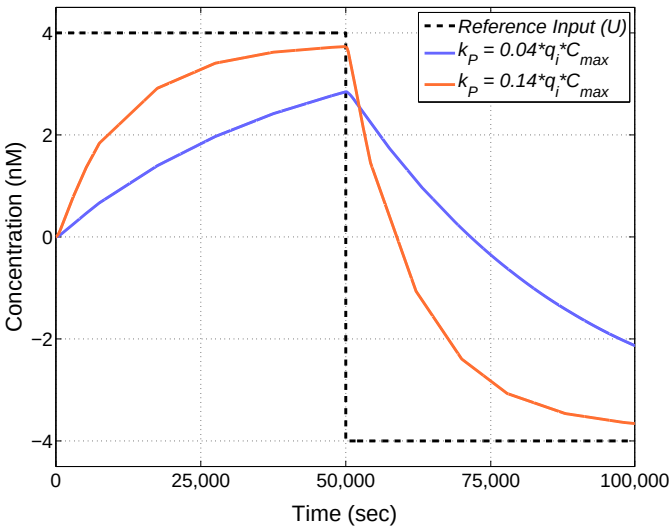

Fig. 14: Closed loop tracking response obtained using the PI controller after accounting for retroactivity effects.

the PI controller is used. The closed loop response dynamics that can be achieved with the PI controller are approximately an order of magnitude slower than those achieved using the QSM controller.

The closed loop responses shown in Figs. 10 and 12 assume perfect modularity of the different elements of the feedback system shown in Fig. 1, i.e. interconnection of elements does not change their dynamic response. Although this assumption is routinely made in the vast majority of systems traditionally encountered in engineering disciplines, it has recently been established that it does not hold for many biomolecular feedback systems, [19], since it often happens that different modules share the same molecular species. The concept of retroactivity has been introduced to quantify the manner in which the interconnection of two modules changes their dynamics with respect to their behaviour when isolated, [20], [21]. For the system under consideration here, it should be noted that the interconnection of modules containing only unimolecular reactions produces no retroactivity effects. For example, in the context of Fig. 1, the interconnection of the subtractor and the PI controller will feature no retroactivity. However, if the system is an interconnection of two modules, one of which comprises unimolecular reactions while the other features bimolecular reactions (e.g. the subtractor and QSM controller) then it will feature a unidirectional retroactivity, since the ODE representation of the subtractor must consider the chemical reactions describing the downstream QSM controller. For the QSM, retroactivity affects the ODEs of two state variables as follows:

$$\frac{dX_1}{dt} = k_s(U-Y-X_1) \underbrace{-k_{b_1}X_1B+k_{c_1}X_2}_{retroactivity}, \quad (31)$$

$$\frac{dA}{dt} = k_{c_1}X_2 - k_{b_2}AX_3 \underbrace{-k_{r_1}AX_5}_{retroactivity}. \quad (32)$$

The additional term $(-k_{b_1}X_1B+k_{c_1}X_2)$ in equation (31) quantifies the retroactivity imposed by the downstream QSM controller on the upstream subtractor through the shared signal X_1, while the additional term $(k_{r_1}AX_5)$ in equation (32) quantifies the retroactivity effects between the QSM controller and the process to be controlled through the shared signal A.

As shown in Fig. 13, the nonlinear QSM controller is highly robust to retroactivity effects, with the major change to the closed loop response being a small reduction in overshoot. In the case of the PI controller, retroactivity affects the ODE of only one state variable, due to the interconnection of the controller and process to be controlled, as follows:

$$\frac{dA}{dt} = k_pX_1 + k_cX_2 - k_dA \underbrace{-k_{r_1}AX_5}_{retroactivity}. \quad (33)$$

As shown in Fig. 14, for the PI controller the presence of retroactivity results in significant changes in the closed loop response, which is now extremely sluggish - for a k_p value of 0.04 q_i C_{max} the controller is not able to track the reference signal even after 50,000 seconds. Understanding the precise structural reasons for the strong robustness to retroactivity effects displayed by the QSM controller is the subject of current research by the authors.

V. CONCLUSIONS AND FUTURE WORK

We have presented new results on how idealized chemical reactions can be used to design and implement an important class of nonlinear controllers using DNA strand displacement. These results exploit bimolecular as well as unimolecular reactions to significantly extend the design framework established for linear dynamical systems in [8], allowing the implementation of highly nonlinear synthetic control circuits based on sliding mode control theory. We have shown how a combination of three elementary abstract idealized reactions, viz., catalysis, annihilation, and degradation can be used to realize all necessary functions and have translated these

chemical reactions into enzyme-free, entropy/enthalpy driven DNA reactions. Simulation results indicate that, compared to a traditional PI controller, the implemented quasi sliding mode controller results are dramatically faster and more accurate in tracking of reference signals, even in the presence of retroactivity. The proposed design approach is highly modular, fully exploits the inherently nonlinear nature of biomolecular reaction kinetics, and makes for the first time a direct link between the biological concept of ultrasensitivity and the engineering theory of sliding mode control.

Several avenues for further research are opened up by this study. For successful implementation of complex feedback control circuits it will be essential to understand the trade-offs between system performance and complexity (particularly in terms of the number of chemical reactions to be implemented experimentally), as well as the effect of experimental uncertainties on closed loop performance (e.g. robustness to variations in reaction rates, etc). It would thus be interesting to investigate whether there are alternative sets of CRNs that could implement a QSM controller using fewer chemical reactions. Sliding mode controllers are only one of many potential nonlinear control schemes that could potentially be implemented using DNA-based chemistry, and much work remains to be done to forge closer links between nonlinear control theory, chemical reaction network theory, and the experimental realities of nucleic acid implementations of complex dynamical systems. The treatment in this paper has focussed on deterministic CRNs, but there has been much recent work on CRNs within a stochastic systems framework that could also be applied in the context of the design of biomolecular controllers. Lastly, while the assumption of well-mixed conditions in *in vitro* systems seems valid, the implementation of DNA-based circuits *in vivo* will require careful consideration of spatial factors, motivating the extension of the underlying design framework to include partial differential equation-based models.

VI. ACKNOWLEDGMENTS

We gratefully acknowledge financial support from EPSRC and BBSRC via research grant BB/M017982/1 and from the School of Engineering of the University of Warwick.

REFERENCES

[1] J. Stapleton, K. Endo, Y. Fujita, K. Hayashi, M. Takinoue, H. Saito, and T. Inoue, "Feedback Control of Protein Expression in Mammalian Cells by Tunable Synthetic Translational Inhibition", *ACS Synthetic Biology*, vol. 1, no. 3, pp. 83–88, 2012.

[2] O. Andries, T. Kitada, K. Bodner, N. Sanders, and R. Weiss, "Synthetic Biology Devices and Circuits for RNA–based 'Smart Vaccines': A Propositional Review", *Expert Review of Vaccines*, vol. 14, no. 2 , pp. 313–331, 2015.

[3] B. Andrews and P. Iglesias, "Control Engineering and Systems Biology" in *Mathematical Methods for Robust and Nonlinear Control*, pp. 267–288. Springer London, 2007.

[4] M. Feinberg, *Lectures on Chemical Reaction Networks, Notes of Lectures Given at the Mathematics Research Center of the University of Wisconsin*, [Online]. Available: http://www.che.eng.ohio-state.edu/ FEINBERG/LecturesOnReactionNetworks, 1979.

[5] M. Bilotta, C. Cosentino, D. G. Bates and F. Amato, "Retroactivity Analysis of a Chemical Reaction Network Module for the Subtraction of Molecular Fluxes", *in Proceedings of the 37th IEEE Engineering in Medicine and Biology Conference*, Milano, 2015.

[6] C. Briat, A. Gupta and M. Khammash, "Antithetic Integral Feedback Ensures Robust Perfect Adaptation in Noisy Biomolecular Networks", *Cell Systems*, vol. 2, no. 1, pp. 15–26, 2016.

[7] C. Briat, A. Gupta and M. Khammash, "Antithetic integral feedback: A New Motif for Robust Perfect Adaptation in Noisy Biomolecular Networks", bioRxiv, doi: http://dx.doi.org/10.1101/024919, 2015.

[8] K. Oishi and E. Klavins, "Biomolecular Implementation of Linear I/O Systems", *IET Systems Biology*, vol. 5, no. 4, pp. 252–260, 2011.

[9] M. Pedersen and B. Yordanov, "Programming Languages for Circuit Design", *Computational Methods in Synthetic Biology*, pp. 81–104, 2014.

[10] B. Yordanov, J. Kim, R. Petersen, A. Shudy, V. Kulkarni and A. Phillips, "Computational Design of Nucleic Acid Feedback Control Circuits", *ACS Synthetic Biology*, vol. 3, no. 8, pp. 600–616, 2014.

[11] D. Soloveichik, G. Seelig and E. Winfree, "DNA as a Universal Substrate for Chemical Kinetics", *Proceedings of the National Academy of Sciences, USA*, vol. 107, no. 12, pp. 5393–5398, 2010.

[12] Y. -J. Chen, N. Dalchau, N. Srinivas, A. Phillips, L. Cardelli, D. Soloveichik and G. Seelig, "Programmable Chemical Controllers made from DNA", *Nature Nanotechnology*, vol. 8, pp. 755762, 2013.

[13] N. Srinivas, T. Ouldridge, P. Šulc, J. Schaeffer, B. Yurke, A. Louis, J. Doye and E. Winfree, "On the Biophysics and Kinetics of Toehold-mediated DNA Strand Displacement", *Nucleic Acids Research*, vol. 41, pp. 10641–10658, 2013.

[14] Y. Shtessel, C. Edwards, L. Fridman, A. Levant, "Introduction: Intuitive Theory of Sliding Mode Control" in *Sliding Mode Control and Observation*, pp. 1–42. Springer New York, 2014.

[15] C. Edwards and S. Spurgeon, "Sliding Mode Control" in *Sliding Mode Control: Theory and Applications*, CRC Press, 1998.

[16] V. Utkin, "Scope of the Theory of Sliding Modes" in *Sliding Modes in Control and Optimization*, pp. 1–11. Springer Berlin Heidelberg, 1992.

[17] H. Khalil, "Nonlinear Design Tools" in *Nonlinear Systems*, pp. 551–625. New Jersey Prentice Hall, 2002.

[18] B. Rauzan, E. McMichael, R. Cave, L. Sevcik, K. Ostrosky, E. Whitman, R. Stegemann, A. Sinclair, M. Serra, A. Deckert, "Kinetics and Thermodynamics of DNA, RNA, and Hybrid Duplex Formation", *Biochemistry*, vol. 52, no. 5, pp. 765–772, 2013.

[19] D. Del Vecchio, A. Ninfa and E. Sontag, "Modular Cell Biology: Retroactivity and Insulation", *Molecular Systems Biology*, vol. 4, no. 1, 2008.

[20] D. Del Vecchio and S. Jayanthi, "Retroactivity Attenuation in Transcriptional Networks: Design and Analysis of an Insulation Device", *Proceedings of IEEE Conference on Decision and Control*, pp. 774–780, Cancun, Mexico, 2008.

[21] S. Jayanthi, K. S. Nilgiriwala and D. Del Vecchio, "Retroactivity Controls the Temporal Dynamics of Gene Transcription" *ACS synthetic biology*, vol. 2, no. 8, pp. 431–441, 2013.

[22] R. Sawlekar, F. Montefusco, V. Kulkarni, and D. G. Bates, "Biomolecular Implementation of a Quasi Sliding Mode Feedback Controller based on DNA Strand Displacement Reactions", *Proceedings of IEEE Engineering in Medicine and Biology Conference*, pp. 949–952. Milan, Italy, 2015.

[23] D. Zhang, "Towards Domain-Based Sequence Design for DNA Strand Displacement Reactions", in *DNA Computing and Molecular Programming*, pp. 162–175. Springer Berlin Heidelberg, 2011.

[24] C. Thachuk, "Logically and Physically Reversible Natural Computing: A Tutorial" in *Reversible Computation*, pp. 247–262. Springer Berlin Heidelberg, 2013.

[25] M. R. Lakin, S. Youssef, F. Polo, S. Emmott and A. Phillips, "Visual DSD: A Design and Analysis Tool for DNA Strand Displacement Systems", *Bioinformatics*, vol. 27, no. 22, pp. 3211–3213, 2011.

[26] D. Zhang and E. Winfree, "Control of DNA Strand Displacement Kinetics using Toehold Exchange", *Journal of the American Chemical Society*, vol. 131, no. 47, pp. 17303–17314, 2009.

[27] J. Watson and F. Crick, "Molecular Structure of Nucleic Acids", *Nature*, vol. 171, no. 4356, pp. 737–738, 1953.

[28] R. Machinek, T. Ouldridge, N. Haley, J. Bath and A. Turberfield, "Programmable Energy Landscapes for Kinetic Control of DNA Strand Displacement", *Nature Communications*, vol. 5, 2014.

[29] A. Goldbeter and D. Koshland, Jr, "An Amplified Sensitivity arising from Covalent modification in Biological Systems", *Proceedings of the National Academy of Sciences, USA*, vol. 78, no. 11, pp. 6840–6844, 1981.

[30] Q. Zhang, S. Bhattacharya and M. Andersen, "Ultrasensitive Response Motifs: Basic Amplifiers in Molecular Signalling Networks", *Open biology* 3, no. 4 : 130031, 2013.

[31] C. Y. Huang, and J. E. Ferrell, Jr., "Ultrasensitivity in the Mitogen-Activated Protein Kinase Cascade", *Proceedings of the National Academy of Sciences, USA*, vol. 93, no. 19, pp. 10078–10083, 1996.

[32] C. Gomez-Uribe, G. C. Verghese and L. A. Mirny, "Operating Regimes of Signaling Cycles: Statics, Dynamics, and Noise Filtering", *PLoS Computational Biology*, vol. 3, no. 12, pp. e246, 2007.

[33] K. J. Astrom and T. Hagglund, "PID Control-Theory, Design and Tuning" in *Advanced PID Control*, ISA - The Instrumentation, Systems, and Automation Society, Research Triangle ParN, NC, 2005.

[34] G. Franklin, J. D. Powell and A. Emami-Naeini, "A First Analysis of Feedback" in *Feedback Control of Dynamic Systems*, Prentice–Hall, 2009.

VII. APPENDIX

Here the DNA implementation reactions, formal CRNs and relevant ODEs for each module of the closed loop feedback control system shown in Fig. 1 are collected and presented in Table IV.

This article has been accepted for publication in a future issue of this journal, but has not been fully edited. Content may change prior to final publication. Citation information: DOI 10.1109/TNB.2016.2560764, IEEE Transactions on NanoBioscience

System Module	DNA Implementation	Formal CRNs	ODEs
(a) QSM Controller	$X_1^\pm + L_1^\pm \underset{q_{max}}{\overset{q_1}{\rightleftharpoons}} H_1^\pm + B_1^\pm$ $B^\pm + H_1^\pm \xrightarrow{q_{max}} O_1^\pm + \phi$ $O_1^\pm + T_1^\pm \xrightarrow{q_{max}} X_2^\pm$	$X_1^\pm + B^\pm \xrightarrow{k_{b_1}} X_2^\pm$	$\frac{dA}{dt} = k_{c_1}X_2 - k_{b_2}AX_3$ $\frac{dX_2}{dt} = k_{b_1}X_1B - k_{c_1}X_2$ $\frac{dX_4}{dt} = k_{b_2}AX_3 - k_{c_2}X_4$ $\frac{dB}{dt} = -k_{b_1}X_1B + k_{c_2}X_4$ $\frac{dX_5}{dt} = -k_{r_1}AX_5 + k_{r_2}X_6$ $\frac{dX_6}{dt} = k_{r_1}AX_5 - k_{r_2}X_6$ $\frac{dY}{dt} = k_{r_2}X_6 - k_{r_3}Y$
	$X_2^\pm + G_2^\pm \xrightarrow{q_2} \phi + O_2^\pm$ $O_2^\pm + T_2^\pm \xrightarrow{q_{max}} A^\pm + X_1^\pm$	$X_2^\pm \xrightarrow{k_{c_1}} A^\pm + X_1^\pm$	
	$X_2^+ + L_3 \underset{q_{max}}{\overset{q_{max}}{\rightleftharpoons}} H_3 + B_3$ $X_2^- + LS_3 \underset{q_{max}}{\overset{q_{max}}{\rightleftharpoons}} HS_3 + BS_3$ $X_2^- + H_3 \xrightarrow{q_{max}} \phi$	$X_2^+ + X_2^- \xrightarrow{\eta} \phi$	
	$A^+ + L_4 \underset{q_{max}}{\overset{q_{max}}{\rightleftharpoons}} H_4 + B_4$ $A^- + LS_4 \underset{q_{max}}{\overset{q_{max}}{\rightleftharpoons}} HS_4 + BS_4$ $A^- + H_4 \xrightarrow{q_{max}} \phi$	$A^+ + A^- \xrightarrow{\eta} \phi$	
	$A^\pm + L_5^\pm \underset{q_{max}}{\overset{q_5}{\rightleftharpoons}} H_5^\pm + B_5^\pm$ $X_3^\pm + H_5^\pm \xrightarrow{q_{max}} O_5^\pm + \phi$ $O_5^\pm + T_5^\pm \xrightarrow{q_{max}} X_4^\pm$	$A^\pm + X_3^\pm \xrightarrow{k_{b_2}} X_4^\pm$	
	$X_4^\pm + G_6^\pm \xrightarrow{q_6} \phi + O_6^\pm$ $O_6^\pm + T_6^\pm \xrightarrow{q_{max}} B^\pm + X_3^\pm$	$X_4^\pm \xrightarrow{k_{c_2}} B^\pm + X_3^\pm$	
	$X_4^+ + LS_7 \underset{q_{max}}{\overset{q_{max}}{\rightleftharpoons}} H_7 + B_7$ $X_4^- + LS_7 \underset{q_{max}}{\overset{q_{max}}{\rightleftharpoons}} HS_7 + BS_7$ $X_4^- + H_7 \xrightarrow{q_{max}} \phi$	$X_4^+ + X_4^- \xrightarrow{\eta} \phi$	
	$B^+ + L_8 \underset{q_{max}}{\overset{q_{max}}{\rightleftharpoons}} H_8 + B_8$ $B^- + LS_8 \underset{q_{max}}{\overset{q_{max}}{\rightleftharpoons}} HS_8 + BS_8$ $B^- + H_8 \xrightarrow{q_{max}} \phi$	$B^+ + B^- \xrightarrow{\eta} \phi$	
(b) Process to be controlled	$A^\pm + L_9^\pm \underset{q_{max}}{\overset{q_9}{\rightleftharpoons}} H_9^\pm + B_9^\pm$ $X_5^\pm + H_9^\pm \xrightarrow{q_{max}} O_9^\pm + \phi$ $O_9^\pm + T_9^\pm \xrightarrow{q_{max}} X_6^\pm$	$A^\pm + X_5^\pm \xrightarrow{k_{r_1}} X_6^\pm$	
	$X_6^\pm + G_{10}^\pm \xrightarrow{q_{10}} \phi + O_{10}^\pm$ $O_{10}^\pm + T_{10}^\pm \xrightarrow{q_{max}} Y^\pm + X_5^\pm$	$X_6^\pm \xrightarrow{k_{r_2}} Y^\pm + X_5^\pm$	
	$Y^\pm + G_{11}^\pm \xrightarrow{q_{11}} \phi$	$Y^\pm \xrightarrow{k_{r_3}} \phi$	
	$Y^+ + L_{12} \underset{q_{max}}{\overset{q_{max}}{\rightleftharpoons}} H_{12} + B_{12}$ $Y^- + LS_{12} \underset{q_{max}}{\overset{q_{max}}{\rightleftharpoons}} HS_{12} + BS_{12}$ $Y^- + H_{12} \xrightarrow{q_{max}} \phi$	$Y^+ + Y^- \xrightarrow{\eta} \phi$	

TABLE IV: DNA implementation reactions, formal CRNs and relevant ODEs : (a) The QSM controller is modelled using 32 DNA implementation reactions that are approximated to 12 formal CRNs. (b) The bimolecular process is modelled using 15 DNA implementation reactions that are approximated to 7 formal CRNs.

This article has been accepted for publication in a future issue of this journal, but has not been fully edited. Content may change prior to final publication. Citation information: DOI 10.1109/TNB.2016.2560764, IEEE Transactions on NanoBioscience

System Module	DNA Implementation	Formal CRNs	ODEs
(c) Subtractor	$U^{\pm} + G_{13}^{\pm} \xrightarrow{q_{13}} \phi + O_{13}^{\pm}$ $O_{13}^{\pm} + T_{13}^{\pm} \xrightarrow{q_{max}} U^{\pm} + X_1^{\pm}$	$U^{\pm} \xrightarrow{k_s} U^{\pm} + X_1^{\pm}$	$\frac{dX_1}{dt} = k_s(U - Y - X_1)$
	$Y^{\pm} + G_{14}^{\pm} \xrightarrow{q_{14}} \phi + O_{14}^{\pm}$ $O_{14}^{\pm} + T_{14}^{\pm} \xrightarrow{q_{max}} Y^{\pm} + X_1^{\mp}$	$Y^{\pm} \xrightarrow{k_s} Y^{\pm} + X_1^{\mp}$	
	$X_1^{\pm} + G_{15}^{\pm} \xrightarrow{q_{15}} \phi$	$X_1^{\pm} \xrightarrow{k_s} \phi$	
	$X_1^{+} + L_{16} \underset{q_{max}}{\overset{q_{max}}{\rightleftharpoons}} H_{16} + B_{16}$ $X_1^{-} + LS_{16} \underset{q_{max}}{\overset{q_{max}}{\rightleftharpoons}} HS_{16} + BS_{16}$ $X_1^{-} + H_{16} \xrightarrow{q_{max}} \phi$	$X_1^{+} + X_1^{-} \xrightarrow{\eta} \phi$	
	$X_1^{+}(0) = 4$ nM $X_1^{-}(50000) = 8$ nM	$X_1^{+}(0) = 8$ nM $X_1^{-}(50000) = 16$ nM	$X_1(t) = \begin{cases} 4 \times 10^{-9} & t \in [0, 50000) \\ -4 \times 10^{-9} & t \in [50000, 100000) \end{cases}$
(d) PI Controller	$X_1^{\pm} + G_{17}^{\pm} \xrightarrow{q_{17}} \phi + O_{17}^{\pm}$ $O_{17}^{\pm} + T_{17}^{\pm} \xrightarrow{q_{max}} X_1^{\pm} + X_2^{\pm}$	$X_1^{\pm} \xrightarrow{k_I} X_1^{\pm} + X_2^{\pm}$	$\underbrace{\frac{dX_2}{dt} = k_I X_1}_{\text{Integration}}$
	$X_2^{+} + L_{18} \underset{q_{max}}{\overset{q_{max}}{\rightleftharpoons}} H_{18} + B_{18}$ $X_2^{-} + LS_{18} \underset{q_{max}}{\overset{q_{max}}{\rightleftharpoons}} HS_{18} + BS_{18}$ $X_2^{-} + H_{18} \xrightarrow{q_{max}} \phi$	$X_2^{+} + X_2^{-} \xrightarrow{\eta} \phi$	
	$X_1^{\pm} + G_{19}^{\pm} \xrightarrow{q_{19}} \phi + O_{19}^{\pm}$ $O_{19}^{\pm} + T_{19}^{\pm} \xrightarrow{q_{max}} X_1^{\pm} + A^{\pm}$	$X_1^{\pm} \xrightarrow{k_P} X_1^{\pm} + A^{\pm}$	$\underbrace{\frac{dA}{dt} = k_p X_1 + k_c X_2 - k_d A}_{\text{Gain}}$
	$X_2^{\pm} + G_{20}^{\pm} \xrightarrow{q_{20}} \phi + O_{20}^{\pm}$ $O_{20}^{\pm} + T_{20}^{\pm} \xrightarrow{q_{max}} X_2^{\pm} + A^{\pm}$	$X_2^{\pm} \xrightarrow{k_c} X_2^{\pm} + A^{\pm}$	
	$A^{\pm} + G_{21}^{\pm} \xrightarrow{q_{21}} \phi$	$A^{\pm} \xrightarrow{k_d} \phi$	
	$A^{+} + L_{22} \underset{q_{max}}{\overset{q_{max}}{\rightleftharpoons}} H_{22} + B_{22}$ $A^{-} + LS_{22} \underset{q_{max}}{\overset{q_{max}}{\rightleftharpoons}} HS_{22} + BS_{22}$ $A^{-} + H_{22} \xrightarrow{q_{max}} \phi$	$A^{+} + A^{-} \xrightarrow{\eta} \phi$	

TABLE IV (contd.): DNA implementation reactions, formal CRNs and relevant ODEs : (c) The subtractor module uses 13 DNA implementation reactions that are approximated to 7 formal CRNs. (d) The PI controller is modelled using 20 DNA implementation reactions that are approximated to 10 formal CRNs.